Identity of the NMDA receptor coagonist is synapse specific and developmentally regulated in the hippocampus

Matildé Le Bail[a], Magalie Martineau[b], Silvia Sacchi[c,d], Natalia Yatsenko[a], Inna Radzishevsky[e], Sandrine Conrod[a], Karima Ait Ouares[a], Herman Wolosker[e], Loredano Pollegioni[c,d], Jean-Marie Billard[f,1], and Jean-Pierre Mothet[a,1,2]

[a]Aix Marseille University, Centre de Recherche en Neurobiologie et Neurophysiologie de Marseiille UMR7286 CNRS, F-13344 Marseille, France; [b]Department of Cellular Biophysics, Institute for Medical Physics and Biophysics, University of Muenster, 48149 Muenster, Germany; [c]Dipartimento di Biotecnologie e Scienze della Vita, Università degli Studi dell'Insubria and [d]The Protein Factory, Politecnico di Milano, Istituto di Chimica del Riconoscimento Molecolare Consiglio Nazionale delle Ricerche Milano, and Università degli Studi dell'Insubria, 21100 Varese, Italy; [e]Department of Biochemistry, The Rappaport Faculty of Medicine and Research Institute, Technion–Israel Institute of Technology, Haifa 31096, Israel; and [f]Center of Psychiatry and Neuroscience, University Paris Descartes, Sorbonne Paris City, UMR 894, 75014 Paris, France

NMDA receptors (NMDARs) require the coagonists D-serine or glycine for their activation, but whether the identity of the coagonist could be synapse specific and developmentally regulated remains elusive. We therefore investigated the contribution of D-serine and glycine by recording NMDAR-mediated responses at hippocampal Schaffer collaterals (SC)–CA1 and medial perforant path–dentate gyrus (mPP–DG) synapses in juvenile and adult rats. Selective depletion of endogenous coagonists with enzymatic scavengers as well as pharmacological inhibition of endogenous D-amino acid oxidase activity revealed that D-serine is the preferred coagonist at SC–CA1 mature synapses, whereas, unexpectedly, glycine is mainly involved at mPP–DG synapses. Nevertheless, both coagonist functions are driven by the levels of synaptic activity as inferred by recording long-term potentiation generated at both connections. This regional compartmentalization in the coagonist identity is associated to different GluN1/GluN2A to GluN1/GluN2B subunit composition of synaptic NMDARs. During postnatal development, the replacement of GluN2B- by GluN2A-containing NMDARs at SC–CA1 synapses parallels a change in the identity of the coagonist from glycine to D-serine. In contrast, NMDARs subunit composition at mPP–DG synapses is not altered and glycine remains the main coagonist throughout postnatal development. Altogether, our observations disclose an unprecedented relationship in the identity of the coagonist not only with the GluN2 subunit composition at synaptic NMDARs but also with astrocyte activity in the developing and mature hippocampus that reconciles the complementary functions of D-serine and glycine in modulating NMDARs during the maturation of tripartite glutamatergic synapses.

NMDA receptors | coagonist | synapse | developmental switch | hippocampus

The glutamate-gated N-methyl-D-aspartate receptors (NMDARs) play a critical role in structural and functional plasticity at synapses during postnatal brain development and in adulthood (1) and are therefore central to many cognitive functions such as learning and memory (2). Disturbances of their functions have been associated to a broad range of neurological and psychiatric disorders (3). NMDARs are heterotetramers typically composed of GluN1 and GluN2 subunits (3, 4), and the precise subunit composition determines NMDAR functional and trafficking properties (3, 4).

NMDARs are unique among neurotransmitter receptors because their activation requires the binding of both glutamate and a coagonist initially thought to be glycine (5, 6). Nevertheless, subsequent studies have shown that D-serine synthesized by serine racemase (SR) (7) would be the preferred endogenous coagonist for synaptic NMDARs in many areas of the mature brain (8), raising controversies about "where, when, and how"

glycine and D-serine might regulate NMDARs at synapses in the brain. This controversy is highlighted by the recent findings showing that D-serine and glycine both released by neurons come into play to regulate synaptic NMDAR-dependent functions at the hippocampal Schaffer collateral (SC)–CA1 synapses of adult brain (9), whereas others found no evidence for a function of glycine at this connection (10). Possible explanations for the relative contribution of D-serine and glycine in gating mature NMDARs were recently given by two recent studies. First, it was shown at hippocampal SC–CA1 synapses that D-serine would target GluN1/GluN2A-containing NMDARs, which are preferentially present within the synapse, whereas glycine would rather target GluN1/GluN2B-containing NMDARs located extrasynaptically (10). Second, it was proposed that the identity of the effective coagonist at synapses could depend on synaptic activity levels with tonic activation of NMDARs under low-activity conditions supported by ambient D-serine, whereas glycine will contribute in response to enhanced afferent activity (11).

So far, most studies have explored the functions of D-serine vs. glycine at excitatory synapses in the adult brain or during aging

Significance

NMDA receptors (NMDARs) support patterning and activity of synapses throughout life and are central to many brain disorders. The NMDAR activation requires the concomitant binding of glutamate and a coagonist glycine or D-serine. To date, whether a preference for one coagonist at specific connections occurs remains unsolved. Here, we sought to determine when and where D-serine and glycine enter into play at hippocampal synapses. We demonstrate that the identity of the NMDAR coagonist is synapse specific and developmentally regulated. Remarkably, this segregation coincides with the subunit composition of postsynaptic NMDARs and the maturation of the tripartite synapse. These results point out the importance of the spatial and temporal switch in coagonist identity for therapeutic interventions aimed at treating deficits in NMDAR activity.
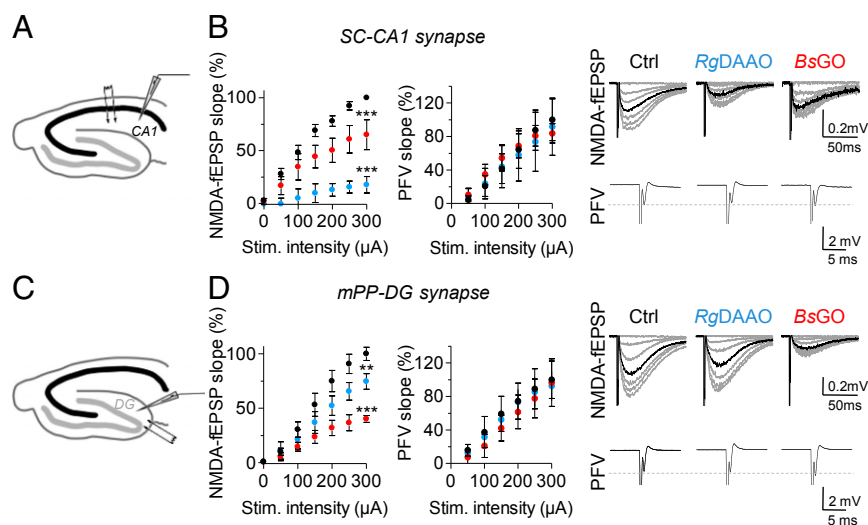
Fig. 1. Relative contribution of D-serine and glycine in the control of synaptic NMDARs at SC–CA1 and mPP–DG excitatory synapses in the mature hippocampus. (A–D) Plotted synaptic input–output curves for NMDA-fEPSPs were obtained in slices at 28–30 °C of 2- to 3-mo-old rats at SC–CA1 (A and B) and mPP–DG synapses (C and D) by presynaptic stimulation of increasing intensity (0–300 μA) in control conditions (Ctrl, black symbols), or in the presence of either *Rg*DAAO (blue symbols) or *Bs*GO (red symbols). NMDA-fEPSPs slope (in millivolts per millisecond) was first normalized to presynaptic fiber volley (PFV) (in millivolts per millisecond) before plotting against stimulation intensity. For CA1 and DG, averaged NMDA-fEPSPs (gray trace) and their corresponding PFV are illustrated on *Right*. The superimposed black traces represent the averaged NMDA-fEPSPs recorded at 75% of maximal amplitude for each condition and in each area. **$P < 0.01$, ***$P < 0.001$ from control using two-way ANOVA. All values represent the mean ± SEM.

(8) where GluN2A-expressing NMDARs prevail (1). Intriguingly, the respective role of the coagonists during postnatal development awaits to be addressed. Considerable evidence indicates that the NMDAR composition at excitatory synapses undergo an experience-dependent developmental switch from primarily GluN2B to GluN2A subunits during the first 2 wk of maturation and refinement of cortical circuits in the postnatal brain (1, 12–14). However, how this developmental switch is controlled is still elusive, and we do not know how it could be regulated or associated to the action of a preferred coagonist.

The present study aimed at investigating the relative synapse specificity and the time window at which D-serine and glycine enter in function to drive NMDAR activity of developing and mature excitatory synapses in the hippocampus. In particular, we sought to elucidate whether the preference for one of the two coagonists could be related to any of the GluN2 subtypes of NMDARs.

Results

The Nature of the Coagonist of Synaptic NMDARs Differs Between SC–CA1 and Medial Perforant Path–Dentate Gyrus Synapses in the Mature Brain.

First, we characterized the respective role of endogenous D-serine and glycine at gating postsynaptic NMDARs in distinct area within the mature hippocampus. To this end, we exploited the use of specific enzymatic scavengers to probe the functions of D-serine and glycine. Application of *Rhodotorula gracilis* D-amino acid oxidase (*Rg*DAAO) (0.2 U/mL) to specifically degrade D-serine substantially reduced by 83.7 ± 5.9% [$F_{(1,133)} = 250.73$; $P < 0.0001$; $n = 6$] NMDAR-mediated field excitatory postsynaptic potentials (NMDA-fEPSPs) recorded at SC–CA1 synapses (Fig. 1 A and B). These responses were only reduced by 35.5 ± 11.5% when endogenous glycine was degraded with a novel highly active variant of *Bacillus subtilis* glycine oxidase (*Bs*GO) (0.2 U/mL) (15) [$F_{(1,140)} = 29.37$; $P < 0.0001$; $n = 7$] (Fig. 1B). *Rg*DAAO or *Bs*GO application did not affect the presynaptic fiber volley (PFV) (Fig. 1B), arguing against an indirect effect on axonal excitability (10, 16). We next investigated the contribution of the two coagonists at medial perforant path–dentate gyrus (mPP–DG) synapses (Fig. 1 C and D). Strikingly, application of *Rg*DAAO at mPP–DG synapses reduced NMDA-fEPSPs but only by 25.5 ± 7.2% [$F_{(1,98)} = 9.76$; $P = 0.0023$; $n = 6$], whereas depletion of glycine by *Bs*GO application produced a more pronounced and consistent 59.9 ± 3.1% decrease [$F_{(1,70)} = 76.63$; $P < 0.0001$; $n = 6$] (Fig. 1D). Inactive variants of *Rg*DAAO and *Bs*GO did not affect NMDA-fEPSPs.

These observations indicated that glycine rather than D-serine is the main endogenous coagonist of NMDARs at mPP–DG synapses, mirroring the situation observed in the CA1 area. This regional segregation could reflect difference in coagonist availability between CA1 and DG. However, neither HPLC analysis for quantifying D-serine (DG/CA1 ratio, 0.98; $P > 0.05$) and glycine (DG/CA1 ratio, 1.24; $P > 0.05$) levels nor Western blot analyses for evaluating SR expression revealed any difference between CA1 and DG areas (see Fig. 4 D and E, and Fig. S1), ruling out the possibility that the regional compartmentalization of D-serine vs. glycine functions is due to difference in the amino acid availability.

Both D-Serine and Glycine Function Depends on the Level of SC–CA1 and mPP–DG Synapse Activity.

The synaptic activation of NMDARs under resting or low-activity conditions by either D-serine or glycine does not anticipate their functions at higher levels of synaptic activity as recently observed in the lateral amygdala (11). We therefore investigated the identity of the coagonist in the activity-dependent activation of NMDARs during long-term potentiation (LTP) induced by high-frequency stimulation at SC–CA1 and mPP–DG synapses. This protocol yielded a long-lasting enhancement of AMPA-fEPSP slope (Fig. 2) that was prevented by blocking NMDARs with the specific antagonist D-2-amino-5-phosphonovalerate (D-AP5) (80 μM) (Fig. S2). As previously reported (10, 17, 18), NMDAR-dependent LTP at SC–CA1 synapses was reduced when treating slices with *Rg*DAAO [$F_{(1,26)} = 8.90$; $P = 0.006$; $n = 15$] (Fig. 2 A and E). Most interestingly, *Rg*DAAO also abolished LTP at mPP–DG synapses [$F_{(1,22)} = 34.7$; $P < 0.0001$; $n = 13$] (Fig. 2 B and F), although baseline neurotransmission assessed by input–output curves remained roughly the same under depletion of D-serine (Fig. 1D) as observed in SR-deficient (SR$^{-/-}$) mice (19). On the other hand, degrading glycine by *Bs*GO treatment also altered LTP at SC–CA1 synapses [$F_{(1,29)} = 4.66$; $P = 0.039$; $n = 15$] (Fig. 2 C and E) and fully occluded it at mPP–DG synapses [$F_{(1,20)} = 10.67$; $P = 0.005$; $n = 11$] (Fig. 2 D and F). LTP impairment induced by *Rg*DAAO or *Bs*GO treatments were reversed when saturating exogenous glycine or D-serine was bath applied on top of the enzymatic scavengers (Fig. 2 E and F, and Fig. S2), further demonstrating that the effects of the enzymes were a direct result of a decreased occupancy of the NMDAR glycine-binding site. These findings establish that both glycine and D-serine are necessary for synaptic plasticity at mature hippocampal synapses and therefore suggest that the contribution of the respective coagonists is regulated by synaptic activity levels at both hippocampal synapses.
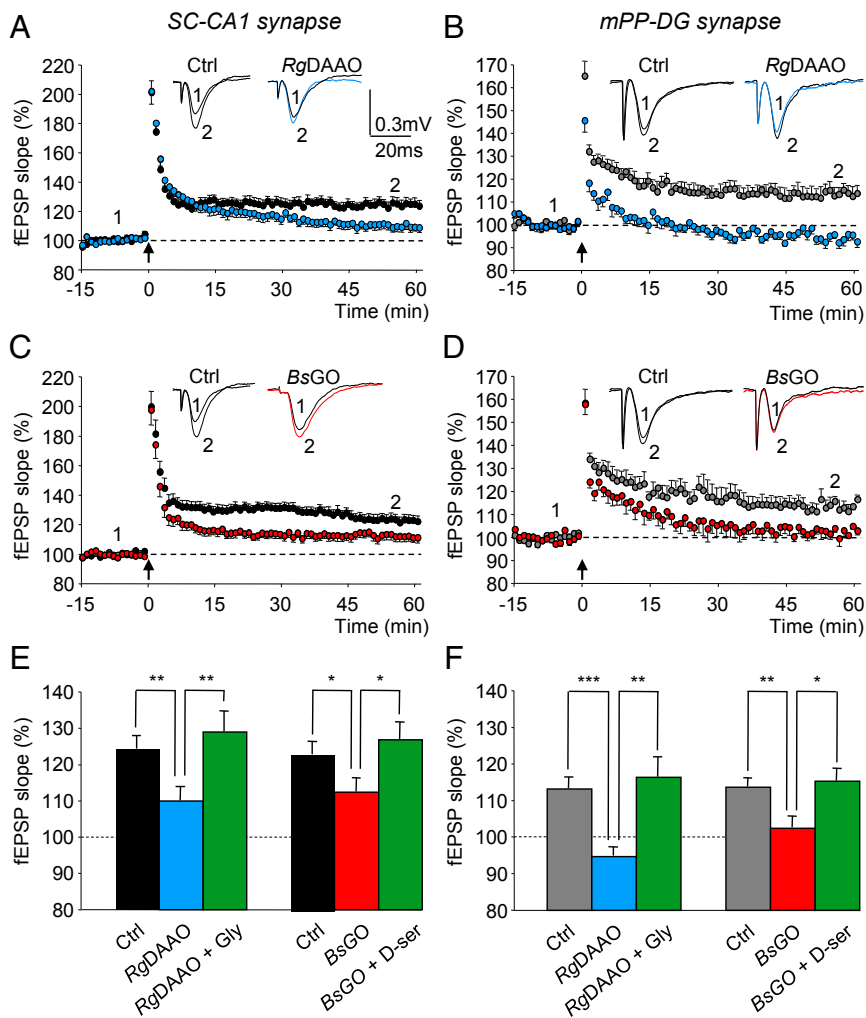
Fig. 2. NMDAR-dependent LTPs at SC–CA1 and mPP–DG excitatory synapses depend on both D-serine and glycine in the mature hippocampus. (*A* and *C*) Time course of LTP induced at SC–CA1 synapses by 1 × 100-Hz conditioning stimulation (arrow) in control slices (black circles) and in slices pretreated with *Rg*DAAO (blue circles) or *Bs*GO (red circles). (*B* and *D*) Time course of LTP induced at mPP–DG synapses by 1 × 100-Hz conditioning stimulation (arrow) in control slices supplied with bicuculline (50 μM) (gray circles) and in slices supplied with bicuculline and pretreated with *Rg*DAAO (blue circles) or *Bs*GO (red circles). For both CA1- and DG-related experiments, *Insets* are superimposed examples of fEPSPs recorded in each condition before (*1*) and 60 min (*2*) after the tetanus. (*E* and *F*) Bar graph illustrating the mean increase ± SEM in fEPSP slope averaged from 45 to 60 min after the conditioning stimulation at SC–CA1 (*E*) and mPP–DG (*F*) synapses in control slices, in slices pretreated with *Rg*DAAO or *Bs*GO and slices pretreated with *Rg*DAAO or *Bs*GO and supplied with either D-serine (100 μM) or glycine (500 μM). *$P < 0.05$, **$P < 0.01$, and ***$P < 0.001$ using one-way ANOVA.

The GluN2 Subunit Composition of SC–CA1 and mPP–DG Synapses Is Different. D-Serine preferentially gates synaptic NMDARs at mature SC–CA1 synapses, whereas glycine favors mPP–DG excitatory synapses. This regional compartmentalization could be the consequence of different GluN2 subunit composition (20) that could favor a synaptic role for either D-serine or glycine (10). We therefore characterized the respective contribution of these different receptor assemblies to synaptic responses using the GluN2B-NMDAR antagonist Ro25-6981 maleate (Ro25-6981) (21) and the GluN2A-NMDAR antagonist zinc (22). We found that Ro25-6981 (2–4 μM) equally weakened NMDA-fEPSPs by 14.6 ± 3.6% ($P = 0.0012$; $n = 15$) at SC–CA1 synapses and by 14.7 ± 6.7% ($P = 0.0107$; $n = 9$) at mPP–DG synapses (Fig. 3). Conversely, free zinc (250–750 nM) more consistently reduced by 33.9 ± 2.9% ($P < 0.0001$; $n = 13$) NMDA-fEPSPs at SC–CA1 synapses, whereas its effect was weaker at mPP–DG synapses (22.9 ± 4.0% decrease; $P = 0.0004$; $n = 10$) (Fig. 3). Increasing the concentrations of Ro25-6981-4 μM and zinc to 750 nM, the maximal doses allowing their specific activity on GluN2B- or GluN2A-NMDARs, respectively (23), did not result in higher

inhibition of NMDA-fEPSPs, showing that inhibition of GluN2A- and GluN2B-NMDARs was already maximal at lower concentrations. Interestingly, the GluN2A/GluN2B ratio obtained with each antagonist (Fig. 3) is lower at mPP–DG synapses (zinc/Ro25-6981; ratio, 1.55) in comparison with SC–CA1 synapses (zinc/Ro25-6981; ratio, 2.32), revealing a stronger contribution of GluN2B- over GluN2A-NMDARs at mPP–DG compared with SC–CA1 synapses. This regional sensitivity revealed by specific subunit pharmacology concorded with the immunoblot analysis that showed a higher expression of GluN2B subunits in DG compared with CA1 (Fig. 4 *B* and *C*, and Fig. S3). Overall, these results indicate that synaptic receptors are predominantly composed of GluN2A-NMDARs at SC–CA1 synapses, whereas GluN2B-NMDARs have a more predominant role at mPP–DG synapses. The different subunit composition between hippocampal synapses parallels their specific coagonist preference (Fig. 1) that further suggests a correlation between the identity of the main coagonist and of the GluN2 subunit composition of synaptic NMDARs.
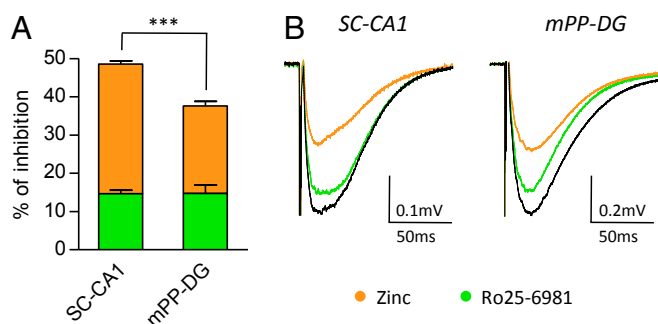
Fig. 3. GluN2A vs. GluN2B subunit composition of NMDARs differs at mature SC–CA1 and mPP–DG synapses. Pharmacological dissection of GluN2A to GluN2B subunits at synapses were obtained using zinc (250–750 nM) and Ro25-6981 (2–4 μM), which are specific GluN2A and GluN2B antagonists, respectively. (*A*) Histogram representing the percentage of inhibition induced by zinc (orange bars) and Ro25-6981 (green bars) at SC–CA1 and mPP–DG synapses after 30 min of perfusion. (*B*) Averaged NMDA-fEPSPs obtained in control (Ctrl, black trace) and under Ro25-6981 or zinc (green and orange traces, respectively) are illustrated. ***$P < 0.001$ using Student *t* test. All values represent the mean ± SEM.

The Nature of the Coagonist Coincides with the Developmental GluN2B-to-GluN2A Subunit Switch at SC–CA1 Synapses. Given the coagonist segregation at mature synapses, we wondered which coagonist could prevail at developing SC–CA1 synapses. Indeed, literature reports a developmental switch in subunit composition from primarily GluN2B- to GluN2A-containing NMDARs during the first 2–3 wk of postnatal maturation at those synapses (1, 12–14). We therefore investigated the relative contribution of the two endogenous coagonists at gating NMDARs at SC–CA1 synapses in hippocampal slices obtained from rats at postnatal day 9 (P9) to P23 when the switch in GluN2 subunits occurs and in adults (P90). Ro25-6981 decreased the NMDA-fEPSPs by $34.0 \pm 4.0\%$ in animals at P9–P10 ($P < 0.0001$; $n = 13$), whereas zinc up to 750 nM had only a weak effect ($17.1 \pm 2.5\%$; $P = 0.0027$; $n = 9$) (Fig. 5*A*). During postnatal development, the antagonist effect of Ro25-6981 progressively decreased, whereas the inhibition by zinc became more prominent, reaching significant respective maximal effects in adulthood ($14.6 \pm 3.6\%$ inhibition for Ro25-6981, $P = 0.0012$, $n = 15$; $33.9 \pm 2.9\%$ inhibition for zinc, $P < 0.0001$, $n = 13$). This functional characterization of a progressive postnatal GluN2B- replacement by GluN2A-NMDARs (Fig. 5*A*) was confirmed by quantitative immunoblot analysis of GluN1, GluN2A, and GluN2B subunits (Fig. 4 *B* and *C*, and Fig. S3). Western blot analysis showed that the expression of GluN2A protein barely detectable at P9–P10 increased by nearly 10- and 18-fold in whole hippocampal and CA1 lysates (see also ref. 13), whereas GluN2B levels showed a moderate and opposite evolution (1.7- and 1.2-fold decrease), significantly rising the GluN2A/GluN2B ratio by ~17- and 22-fold ($P < 0.001$; $n = 7$) across development. Although GluN2B and GluN2A are developmentally regulated, we found that GluN1 protein expression remained unaltered (Fig. 4*B*).

To specify the nature of the coagonist acting at synaptic NMDARs in the developing CA1 area, enzymatic scavengers were applied on hippocampal slices from P9 to P90 rats (Fig. 5*B*). Contrasting with the observed situation in adult animals, *Rg*DAAO did not affect NMDA-fEPSPs in P9–P10 rats ($2.0 \pm 4.8\%$ inhibition; $P = 0.6543$; $n = 12$), whereas responses were strongly reduced by $70.7 \pm 4.2\%$ when endogenous glycine was degraded with *Bs*GO ($P < 0.0001$; $n = 10$) (Fig. 5*B*). A significant inhibitory effect of *Rg*DAAO on NMDA-fEPSPs was progressively detected during development, reaching ~40% of control at P22–P23 ($P = 0.0008$; $n = 5$) and ~83% at P90 ($P = 0.0003$; $n = 6$). In parallel, *Bs*GO inhibitory action significantly diminished

after P12–P14 (Fig. 5*B*). Further analysis of maximal percentage inhibition comparing the effects of zinc and Ro25-6981 together with the effects of *Bs*GO and *Rg*DAAO revealed that D-serine is replacing glycine as the main endogenous coagonist of NMDARs at SC–CA1 synapses after completion of the first 3 wk of postnatal development (Fig. 5*C*). It also revealed the existence of a time window during postnatal development (fourth week) when both glycine and D-serine might serve as coagonists for NMDARs because their depletion results in a ~1:1 inhibition ratio of NMDA-fEPSPs. This progressive switch in the identity of the coagonist tightly paralleled the replacement of GluN2B- by GluN2A-NMDARs (Fig. 4*C*).

Because the relative affinity and potency of glycine and D-serine for GluN2B- and GluN2A-NMDARs is roughly the same (24, 25), we performed HPLC analysis to check whether postnatal changes in coagonist availability could explain the coagonist and NMDAR subunit replacement. HPLC analysis from P10 and P90 hippocampal slices revealed that the levels of glycine are similar in pups and adults (−13% in adult; $P > 0.05$), whereas D-serine content increased by 96% over the same period (Fig. 4*E*), rising significantly the D-serine/glycine ratio by 217% across development (D-serine/glycine ratio is 0.22 ± 0.02 and 0.47 ± 0.06 in young and adult animals, respectively; $P < 0.001$; $n = 8$–10 analyses), thus supporting the developmental switch of their functions. Nevertheless, quantitative Western blot analyses revealed that the expression of SR in the CA1 area did not change significantly during the same postnatal period (Fig. S1), showing that the glycine to D-serine change is not explained by metabolic changes favoring D-serine.

Glycine Is the Main Coagonist at mPP–DG Synapse Throughout Postnatal Development. We next investigated whether the switch of GluN2 subunit and of coagonist identity is a general property of hippocampal synapses by analyzing the developing mPP–DG synapses (Fig. 6). In line with the SC–CA1 synapses, the inhibitory effect of Ro25-6981 significantly decreased by 48.6% at mPP–DG synapses between P9–P10 and P90 ($30.3 \pm 5.5\%$ and $14.7 \pm 6.7\%$, respectively; $P = 0.0001$; $n = 8$–9). However, the effect of zinc remained stable over the same period ($P = 0.3360$; $n = 8$–10), increasing by 35% the specific contribution of GluN2A to the total GluN2A/GluN2B-dependent NMDA-fEPSPs (Fig. 6*A*). In parallel, the contribution of D-serine increased as inferred by the greater inhibition observed with *Rg*DAAO between P9–P10 and P90 ($5.2 \pm 4.2\%$ and $30.2 \pm 8.9\%$, respectively; $P < 0.0001$; $n = 6$), whereas the inhibition by *Bs*GO was stable (Fig. 6*B*). There is thus a concordance in the increasing role of GluN2A and D-serine during postnatal development of mPP–DG synapses, reminiscent of the situation at the SC–CA1 synapses. However, it has to be emphasized that, although the role of D-serine increases postnatally in DG, glycine remains the main endogenous coagonist of NMDARs from P9 to P90 at this location.

The functional analysis of NMDAR activity and coagonist identity were further strengthened by quantitative immunoblot and HPLC analysis. Although the ratio of GluN2A/GluN2B expression tended to increase, yet not significantly (Fig. 4 *B* and *C*), the ratio of D-serine/glycine rose by 148% from P10 to P90 ($P < 0.05$; $n = 10$–15) (Fig. 4*E*). Both coagonist concentrations increased from neonatal period to adulthood. Nevertheless, the increase in D-serine concentration (~340%) was more pronounced than the increase in glycine concentration (~240%) (Fig. 4*E*), explaining the expanding role of D-serine during development without taking over the role of glycine as the main NMDAR coagonist at mPP–DG synapses (Fig. 6).

Contribution of DAAO to the Regional and Developmental Function of D-Serine. We further tested the apparent postnatal switch in coagonist preference at SC–CA1 synapses by a pharmacological approach aiming to target endogenous DAAO and determine
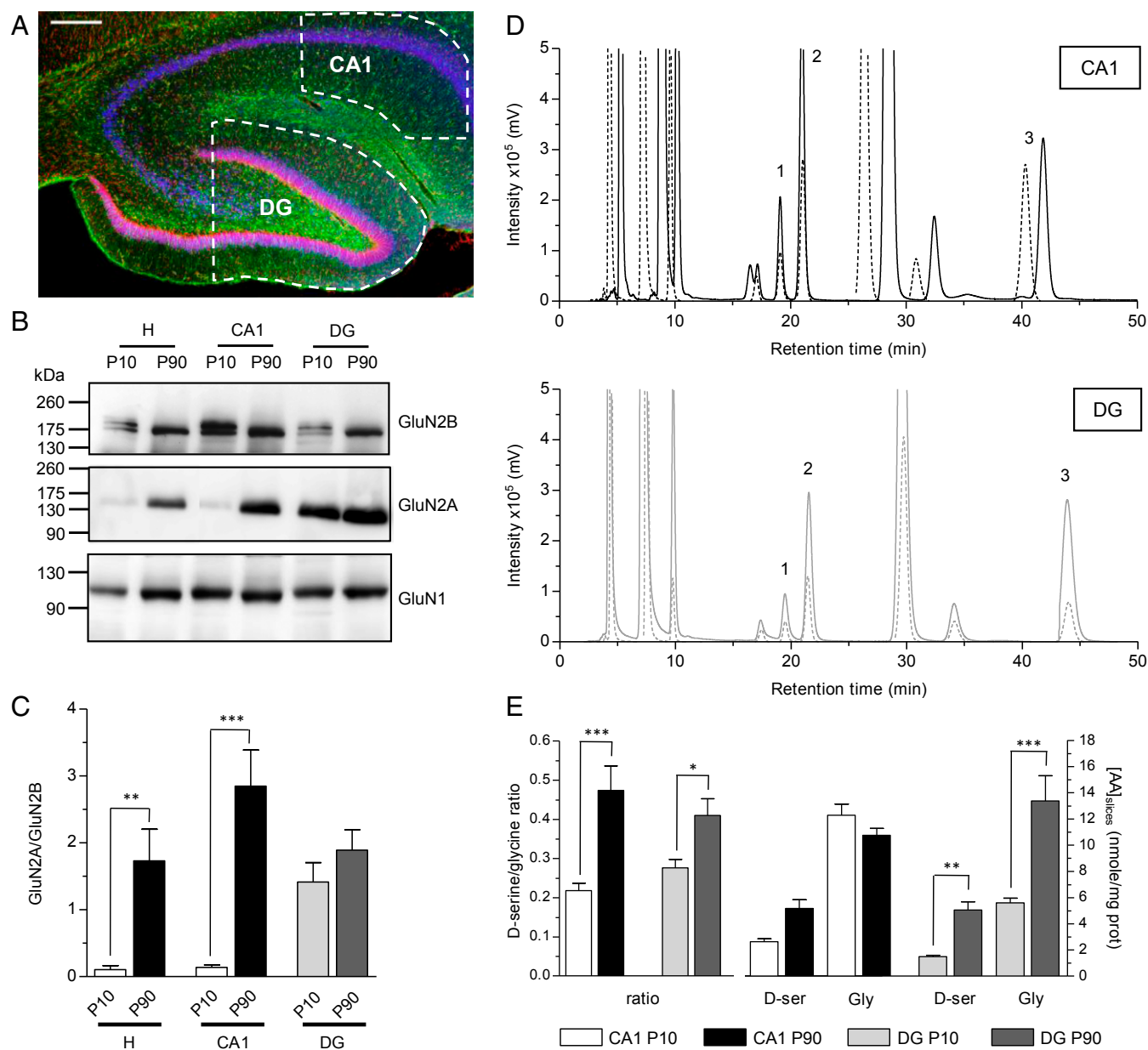
Le Bail et al.

Fig. 4. Parallel regional and developmental switch in GluN2 subunit composition of NMDARs and of coagonists levels. (*A*) Confocal microscopy analysis of hippocampal slice from a P90 rat illustrating the immunostainings of GFAP (green) and NeuN (Red) together with DAPI (blue) staining. CA1 and DG areas isolated by microdissection and used for Western blots and HPLC analysis are indicated by white dashed lines. (Scale bar: 200 μm.) (*B*) Western blot analysis showing the expression of GluN2A, GluN2B, and GluN1 in the whole hippocampus (H), the CA1 and DG areas in P9–P10 and P90 rats. Representative immunoblots are shown for each targeted protein. Signal intensity was measured for each protein, averaged, and plotted. (*C*) The histogram displayed the mean ± SEM values (*n* = 7) of the GluN2A/GluN2B ratio, but see Fig. S3 for the histograms displaying GluN2A/GluN1 and GluN2B/GluN1 ratio. (*D*) Examples of HPLC chromatograms illustrating the detection of D-serine (*1*), L-serine (*2*), and glycine (*3*) obtained from P10 (dashed line) and P90 (plain line) hippocampal CA1 (*Top*) and DG slices (*Bottom*). The identity of the peaks corresponding to D-serine (19.37 ± 0.18 min), L-serine (21.34 ± 0.18 min), and glycine (43.78 ± 0.44 min) were verified by the addition of external standards to the samples, before derivatization. Retention time values are reported as mean ± SEM, *n* = 45 (total slices analyzed). Fluorescence signals were quantified for D-serine, L-serine, and glycine. (*E*) Average contents of glycine, D-serine, and D-serine/glycine ratio across development. The left histogram represents the D-serine/glycine ratio, and the right histogram represents the amino acid (AA) concentrations (in nanomoles per milligram of protein). The histogram bars displayed the mean intensity ± SEM values in CA1 and DG at P10 and P90. *$P < 0.05$, **$P < 0.01$, and ***$P < 0.001$ using one-way ANOVA.

whether this peroxisomal enzyme (26) could control the synaptic availability of D-serine. To this end, we took advantage of the developed series of selective DAAO inhibitors and selected 5-chloro-benzo[*d*]isoxazol-3-ol (CBIO) (27) to probe the role of DAAO in controlling D-serine availability and thus in modulating NMDAR functions. As shown in Fig. 7 *A* and *B*, CBIO (1 μM) increased NMDA-fEPSPs at SC–CA1 synapses in adult animals by 135.6 ± 35.4% ($P = 0.006$; *n* = 8). This potentiating effect of CBIO at

mature SC–CA1 synapse resulted from gain of function of D-serine at NMDARs. Indeed, *Rg*DAAO or zinc treatment either to degrade D-serine or to block any neuromodulation through GluN2A-NMDARs prevented the effect of CBIO (Fig. S4 *A* and *B*). The preventing effect of *Rg*DAAO is not due to the metabolism of CBIO by *Rg*DAAO because CBIO is not a substrate for the recombinant enzyme (Fig. S4*C*). Furthermore, CBIO failed to potentiate NMDA-fEPSPs in SR$^{-/-}$ mice, whereas it consistently
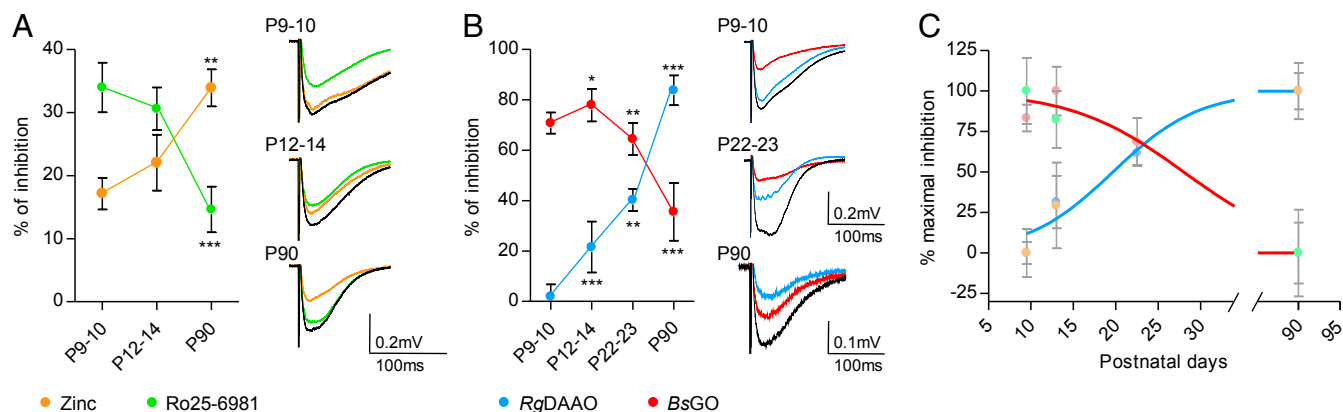
www.manaraa.com

Fig. 5. The identity of the coagonist is associated to the availability of GluN2A vs. GluN2B subunits at SC–CA1 excitatory synapses. (A) Inhibitory effect of zinc (250–750 nM; orange symbols) and Ro25-6981 (2–4 µM; green symbols) at SC–CA1 synapses throughout development (P9–P10, P12–P14, and P90). Corresponding average NMDA-fEPSP traces are illustrated on *Right*. (B) Inhibitory effect of *Rg*DAAO (0.2 U/mL; blue symbols) and *Bs*GO (0.2 U/mL; red symbols) during maturation (P9–P10, P12–P14, P22–P23, and P90). Corresponding average NMDA-fEPSP traces are represented on *Right*. (C) Data from A and B are normalized to the minimal and maximal inhibitory effects. The inhibitory effects of *Rg*DAAO and *Bs*GO are fitted with a sigmoidal dose–response curve (R^2 = 0.9539 and 0.9641, respectively). *$P < 0.05$, **$P < 0.01$, and ***$P < 0.001$, using Student t test when comparing with previous developmental stage. All values represent the mean $\pm$ SEM.

increased the field potentials in wild-type littermates (Fig. S4D). Interestingly, CBIO only produced a slight although significant increase (14.6 $\pm$ 3.3%; $P = 0.0045$; $n = 7$) of NMDA-fEPSPs at mPP–DG synapses (Fig. 7 A and B) in line with our experiments showing that D-serine was not the main endogenous coagonist of NMDARs at these synapses. Finally, we tested the effect of CBIO on NMDA-fEPSPs at immature SC–CA1 synapses and found that the DAAO inhibitor did not affect the responses (1.5 $\pm$ 7.2%; $P = 0.7992$; $n = 8$) (Fig. 7 C and D). Interestingly, DAAO is expressed early during postnatal development as reported earlier (28, 29), and its expression is barely stable across postnatal development. Altogether, these results indicate that pharmacological inhibition of DAAO significantly impacts NMDAR only at ages when D-serine fulfills the role of the main coagonist and not when glycine predominates, confirming that the developmental switch in the nature of the main coagonist is not controlled by the metabolism of D-serine.

A Proper Astrocyte–Neuron Coupling Profiles the Identity of the Coagonist at SC–CA1 Synapses. We next investigated the putative contribution of astrocyte–neuron coupling in the developmental

switch from glycine to D-serine as the coagonist gating NMDARs at SC–CA1 synapses. Astrocytes are key partners for synaptic functions (30, 31) that tightly contribute to the metabolism and the synaptic disposition of D-serine and glycine and therefore their functions (11, 16, 32, 33). We thus hypothesized that structural remodeling of astrocytes at synapses may be involved in this developmental switch by promoting the progressive supply of D-serine at synaptic sites and accelerating glycine clearance through GlyT1 transporters. We first functionally inactivated astrocytes by treating hippocampal slices with the gliotoxin, fluoroacetate (FAC) (5 mM) (16, 30, 34). FAC decreased by 23.6 $\pm$ 8.4% NMDA-fEPSPs ($P = 0.0312$; $n = 7$) recorded at mature SC–CA1 synapses (Fig. 8A) as previously reported (16, 30, 34). Exogenously applied L-serine (200 µM) to silence the effects of FAC consistently rescued NMDA-fEPSPs to control value (108.6 $\pm$ 18.1%; $P = 0.6680$ vs. Ctrl; $n = 6$) (Fig. 8A), showing that the function of NMDARs was not directly affected by the gliotoxin. Interestingly, FAC treatment in P9–P14 rats failed to impact NMDA-fEPSPs (108.4 $\pm$ 6.7%; $P = 0.1616$; $n = 7$), and application of L-serine never potentiated these responses (105.5 $\pm$ 5.6%;
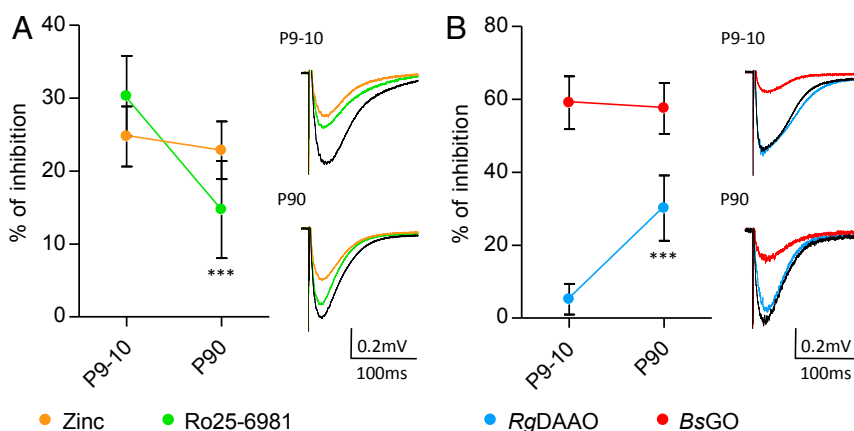

Fig. 6. At mPP–DG synapses, glycine is the preferred coagonist throughout development. (A) Inhibitory effect of zinc (250–750 nM; orange symbols) and Ro25-6981 (2–4 µM; green symbols) at mPP–DG synapses between P9–P10 and P90. Corresponding average NMDA-fEPSP traces are illustrated on *Right*. (B) Inhibitory effect of *Rg*DAAO (0.2 U/mL; blue symbols) and *Bs*GO (0.2 U/mL; red symbols) between P9–P10 and P90. Corresponding average NMDA-fEPSP traces are represented on *Right*. ***$P < 0.001$ using Student t test. All values represent the mean $\pm$ SEM.
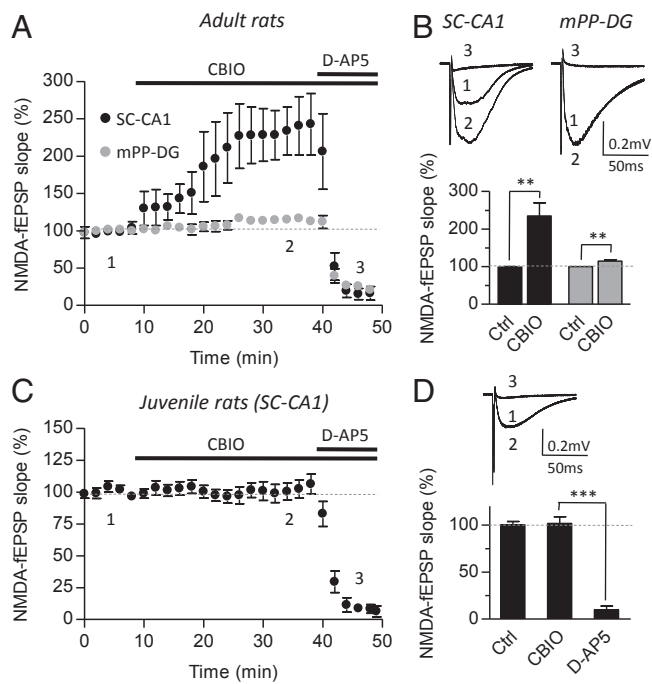
Le Bail et al.

www.manaraa.com

Fig. 7. Gain of function of D-serine through D-amino acid oxidase inhibition displays regional and developmental features. Activity of DAAO was pharmacologically inhibited using CBIO (1 μM). (*A* and *B*) Effects of CBIO at SC–CA1 and mPP–DG synapses in the adult hippocampus. (*A*) For direct comparison between CA1 (black symbols) and DG (gray symbols), averaged and normalized time-courses were plotted for NMDA-fEPSPs recorded in the absence (Ctrl), or in the presence of CBIO alone or in the presence of D-AP5 to block NMDARs. (*B*) Average traces (*Top*) for NMDA-fEPSP obtained in each condition (Ctrl: *1*), CBIO (*2*), and D-AP5 (*3*) are displayed. Summary of experiments in Ctrl and CBIO conditions at SC–CA1 and mPP–DG synapses (*Bottom*). (*C* and *D*) Absence of potentiating effects of CBIO at SC–CA1 synapses from the juvenile hippocampus. NMDA-fEPSPs were recorded as for adult synapses in the absence (Ctrl, *1*), in the presence of CBIO (*2*) and D-AP5 (*3*). **$P < 0.01$ and ***$P < 0.001$ using Student t test. All values represent the mean ± SEM values.

$P = 0.3972$ vs. Ctrl; $n = 6$) (Fig. 8*B*). The contribution of astrocytes was also evaluated by blocking the activity of GlyT1 transporters with *N*-[3-(4′-fluorophenyl)-3-(4′-phenylphenoxy)propyl]sarcosine hydrochloride (ALX5407) (10, 35, 36). Interestingly, bath-applied ALX5407 (1 μM) induced a consistent potentiation of NMDA-fEPSPs at mature SC–CA1 (52.6 ± 10.3%; $P = 0.0035$; $n = 15$) but not at juvenile synapses (5.8 ± 1.7%; $P = 0.1065$; $n = 8$) (Fig. 8 *C* and *D*). Finally, these data demonstrate that the presence of astrocyte at SC–CA1 mature synapses is essential to clear the synapse from glycine and ensure the accessibility of D-serine, thus emphasizing the role of astrocyte–neuron coupling in the developmental switch of NMDAR coagonist.

Discussion

Because proper occupation of the glycine-modulatory site by coagonists is an absolute condition for optimal NMDAR-related synaptic functions, this fundamental feature of the glutamatergic receptor has gained intensive interest, and this binding site is now seen as a primary therapeutic target for improving cognition and associated symptoms in psychiatric and neurological disorders including schizophrenia but also aging (19, 37, 38). However, despite intensive research on the functions of D-serine and glycine at NMDARs, the time and place in which these endogenous coagonists are respectively engaged in modulating synapse activity remains elusive. In this study, selective enzymatic depletion of either endogenous D-serine or glycine as well as

pharmacological inhibition of D-serine–degrading enzyme indicate that, although both amino acids are engaged at hippocampal connections during sustained synaptic activity as also observed in the lateral amygdala (11), D-serine is the preferred coagonist for NMDARs at mature SC–CA1 synapses, whereas unexpectedly this role is assumed by glycine at mPP–DG synapses under basal synaptic activity. This regional segregation in the preference of the coagonist identity is closely associated to a specific subtype of GluN1/GluN2A- and GluN1/GluN2B-containing synaptic NMDARs, as revealed by both electrophysiological recordings and by biochemical assays for protein expression. In addition, we reveal that the identity of the coagonist changes during postnatal development at SC–CA1 synapses from glycine in juvenile rats to D-serine in adults, and tightly parallels the described replacement of GluN2B- by GluN2A-NMDAR (1, 12–14). Noteworthy, this developmental switch in GluN2B- to GluN2A-NMDARs and in the identity of the coagonist does not occur at mPP–DG synapses where glycine remains the main coagonist over D-serine throughout postnatal development. This latter observation is in concord with the moderate impairment of NMDAR-dependent activity of DG granule cells in $SR^{-/-}$ mice (19). The onset when D-serine and glycine come into play during postnatal development is of particular interest because NMDARs play a critical role in the refinement and maturation of central synapses prevailing during postnatal development (39, 40).

One possible explanation for the regional and temporal segregation of D-serine and glycine could be a differential NMDAR subunit composition at synapses. Indeed, D-serine was shown to bind NMDARs in brain areas where synapses are mainly formed of GluN2A-containing NMDARs, whereas glycine would target GluN2B-containing receptors (10, 16). Accordingly, we found here that glycine is mainly concerned at synapses of DG and immature CA1 that have greater contribution of GluN2B compared with mature CA1 (see also ref. 20). Conversely, D-serine is involved at synapses of mature CA1 where the contribution of GluN2A is greatly increased. The underlying molecular mechanisms for such preference are not known. It is most unlikely that NMDAR subtypes could discriminate between both amino acids because of better affinity. Indeed, although glycine has a ~10-fold higher affinity for GluN2B-containing NMDARs, D-serine only displays a marginal preference for GluN2A-NMDARs (24, 25, 41). Furthermore, D-serine and not glycine is the main coagonist in the supraoptic nucleus of the hypothalamus where synaptic NMDARs mainly contain the GluN2B subunit (42). Additionally, it has to be mentioned that the amplitudes of enzymatic depletion of endogenous coagonists do not exactly match the amplitudes of pharmacological inhibition of the NMDAR subunits. These observations support the possibility that a fraction of synaptic NMDARs could be GluN2A-GluN2B heterotrimeric at both synapses as recently evidenced notably in the hippocampus (20, 23, 43, 44). Because, those assemblies are expected to be equally affected by both enzymatic and pharmacological approaches, more adequate tools are yet needed to evaluate the regulation of these heterotrimeric receptors by specific coagonist.

Alternatively, the preference for one coagonist could be related to its confined metabolism within defined hippocampal area. However, glycine is essential for all vital functions and its metabolism has to be maintained throughout the life span. Conversely, D-serine is not an essential amino acid *sensu stricto* for metabolic and basic cellular functions. Then, it seems more conceivable that small alterations in the expression of the two enzymes involved in D-serine metabolism could affect its local concentration and thus synaptic activity. In line with this idea, the developmental switch from GluN2B- to GluN2A-NMDARs at SC–CA1 synapses could be regulated by the replacement of glycine by D-serine used as the endogenous coagonist. However, this notion is difficult to reconcile with the findings that D-serine is already present in the brain early after birth (28, 29, 45–47).
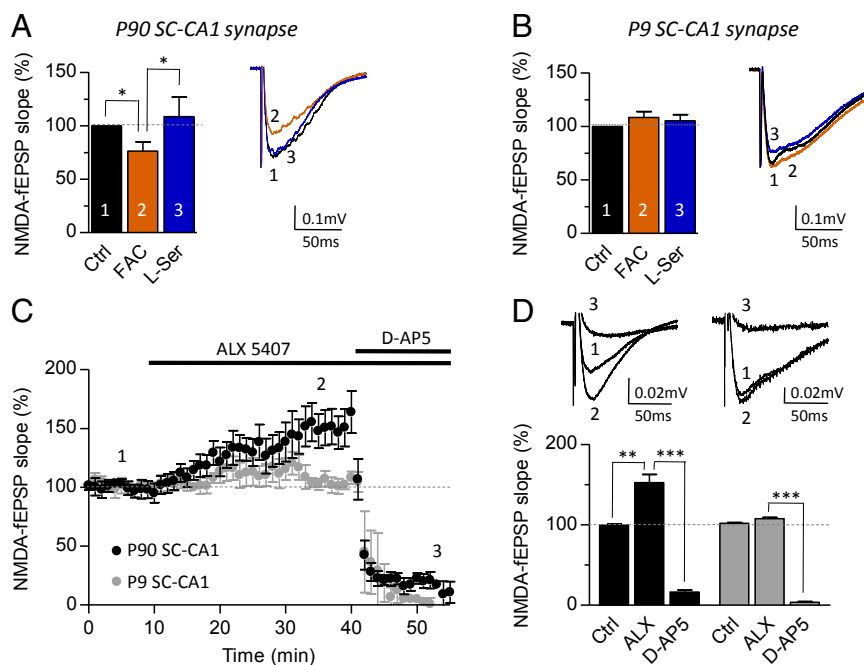
Fig. 8. Developmental contribution of astrocyte to D-serine and glycine synaptic functions. Astrocytes metabolism in P60–P90 (*A*) and P9–P14 (*B*) rats was inhibited by FAC (5 mM; 45 min) at SC–CA1 synapses. Bar graphs represent the effect of FAC (brown column) and L-serine (200 µM; blue column). For adult and juvenile rats, superimposed traces of control (black trace, *1*), FAC (brown trace, *2*) and L-serine (blue trace, *3*) are illustrated on *Right*. (*C*) GlyT1 transporters were inhibited by supplementation with ALX5407 (1 µM) to adult (black symbols) and juvenile (gray symbols) hippocampal slices. Time course of the effect of ALX5407 and D-AP5 (50 µM) on NMDA-fEPSPs were normalized and plotted for direct comparison. (*D*) Bar graph representing the effect of ALX5407 and D-AP5 on adult and juvenile rats. Respective superimposed traces of control (*1*), ALX (*2*), and D-AP5 (*3*) are illustrated on *Top*. *$P < 0.05$, **$P < 0.01$, and ***$P < 0.001$ using Student *t* test. All values represent the mean ± SEM.

Additionally, we now report that its metabolic pathway is not subjected to dramatic regulation during postnatal development of hippocampus, although we observed a trend for an increase in SR expression in striking contrast with the retina (48), the cerebral cortex (49), or the vestibular nuclei (28). In concord with our observations, the $SR^{-/-}$ mice show only partial deficits in cognitive functions but have normal growth and do not show any evident cytoarchitecture abnormality, although the dendritic spine density is altered (19). Still, D-serine levels are developmentally regulated reaching gradually the adult levels during the first 2–3 wk (ref. 49 and herein), supporting the idea that the coagonist would enter only progressively in synaptic function during the postnatal development of forebrain.

On the other hand, the presence of either D-serine or glycine in the synaptic cleft could influence the synaptic composition of NMDARs. In fact, constitutive hypoactivation of NMDARs in the $SR^{-/-}$ mice increases GluN1 and GluN2A subunits in the postsynaptic density (50), whereas gain of function of D-serine by shRNA-mediated DAAO knockdown in the cerebellum decreases GluN2A mRNA (51). On the opposite, overstimulation of NMDARs in $GlyT1^{+/-}$ mice also leads to elevated protein expression of GluN1 and GluN2A (50). These changes in the molecular composition of NMDARs could also occur faster under acute presence/absence of D-serine or glycine. Indeed, the coagonist binding can prime the recycling of NMDARs (52) but also impact their lateral trafficking and confines receptors to distinct functional pools (10). We recently showed that D-serine binding to NMDARs will slow down insertion of GluN2B-NMDARs to the synapse, whereas glycine would strongly inhibit the motility of GluN2A-NMDARs (10). Future studies will need to explore the relative contribution of D-serine and glycine in the trafficking of NMDAR subunits in physiological conditions to understand whether the GluN2B-GluN2A switch

observed at mature synapses and during LTP could be influenced by the coagonists.

Because glycine and D-serine can influence the trafficking and recycling of NMDARs, differences in the processes controlling their synaptic turnover could explain the regional and temporal segregation of coagonists and receptor subunits. D-Serine and glycine synaptic turnover relies on a fine coupling between astrocytes and neurons (33). D-Serine is most likely released by astrocytes via Ca^{2+}-regulated exocytosis (33, 53, 54), whereas the release of glycine would operate principally through the reversal of GlyT1 (55, 56). Neurons contribute to release D-serine and glycine by alanine–serine–cysteine transporter-1 (Asc-1) that locally modulates synaptic NMDARs (9). Unfortunately, we do not know yet how these different neuronal and glial mechanisms may differ or overlap to control the synaptic availability of D-serine and glycine in the CA1 and DG. Nevertheless, the coagonist synaptic turnover would most likely be affected by postnatal development. However, most glial cells in rodents only start to establish appropriate contact with neurons 2–3 wk after birth (57). Interestingly, this timing coincides with the period at which we report that D-serine enters into play at regulating NMDARs. Glycine levels are mainly regulated by GlyT1 transporters that show highly regulated pattern of expression and activity across development (36). Thus, low activity of GlyT1 together with weak neuro-glial coupling at synapses during early phase of development would favor predominant glycine availability in synaptic cleft. Accordingly, we demonstrated the role of astrocytes in maintaining a proper synaptic activity during adulthood. In light of our results, we propose that the formation of functional tripartite synapses during the first weeks of postnatal development (57) promotes the progressive activation of the neuro-glial D-serine shuttle (32, 33) supplying the coagonist at synaptic sites while favoring glycine clearance through GlyT1 transporters (36). This would result in a reduced diffusion and

Le Bail et al.

retention of GluN2B-NMDARs in the synaptic environment, leading to their replacement by GluN2A-NMDARs. Accordingly, we propose that glycine would be a better coagonist of immature and developing synapses, whereas D-serine function would be an index of more mature synapses. This scenario perfectly fits with the fact that the DG is one of the few brain regions exhibiting adult neurogenesis where newborn neurons are integrated into neuronal circuits (58). The DG where glycine is favored as a coagonist is somewhat a more immature structure even at adulthood compared with the CA1 area where D-serine is preferentially acting, without excluding a function of D-serine in adult neurogenesis as recently reported (58).

What is the physiological outcome of a developmental substitution from glycine to D-serine at SC–CA1 synapses and what is the physiological need for synapse to use preferentially one specific coagonist even within the same cerebral area are two questions that remain to be answered before elaborating new pharmacological strategies aimed at reducing NMDAR-dependent neuronal dysfunction.

Materials and Methods

Further details on materials, electrophysiology, HPLC, and immunostaining analysis can be found in *SI Materials and Methods*.

Animals. Animals were bred in house in polycarbonate cages and maintained on a 12/12-h light/dark cycle in a temperature (22 °C)- and humidity-controlled room. Animals were given access to food and water ad libitum. All experiments were conducted in accordance with European and French directives on animal experimentation and were approved by the INSERM, CNRS, and Aix-Marseille University animal care committees.

Electrophysiology. P9–P23 and 2- to 3-mo-old rats were decapitated under isoflurane anesthesia. The brain was quickly removed from the skull and maintained in ice-cold artificial cerebrospinal fluid (ACSF) oxygenated with 95% (vol/vol) O_2 and 5% CO_2 (pH 7.3–7.4) containing the following (in mM): 123 NaCl, 2.5 KCl, 1.3 NaH_2PO_4, 26.2 $NaHCO_3$, 1.3 $MgCl_2$, 2.5 $CaCl_2$, and 10 glucose. Coronal hippocampal slices (350 μm thick) were prepared and incubated during 30 min at 30 °C in oxygenated ACSF containing 2.5 mM Mg^{2+} and 1 mM Ca^{2+}. After incubation, slices recovered at room temperature for at least 30 min and were then transferred in a recording chamber continuously perfused with 28–30 °C and oxygenated ACSF at a flow rate of 2 mL/min. fEPSPs were evoked by a 0.033-Hz stimulation through a bipolar stimulating electrode and recorded using a glass pipette (3–5 MΩ) filled with ACSF. NMDA-fEPSPs were isolated in low-Mg^{2+} ACSF (0.1–0.2 mM) containing picrotoxin (50 μM) and 2,3-dihydroxy-6-nitro-7-sulfamoyl-benzo[*f*]quinoxaline-2,3-dione (NBQX) (10 μM) to block GABA and AMPA/kainate receptors, respectively. NMDA-fEPSPs at SC–CA1 synapses were recorded in the stratum radiatum in response to the stimulation of the SCs (9, 10). NMDA-fEPSPs in the DG were recorded in the stratum moleculare following stimulation of the mPP fibers (19, 59). The initial slope of the EPSP rising phase was used to measure the changes in synaptic strength. Recordings were obtained using an Axon Multiclamp 700B amplifier (Molecular Devices), sampled at 20 kHz, filtered at 2 kHz, and analyzed using pClamp10

software (Molecular Devices). Average NMDA-fEPSPs traces were obtained from at least 10 min of stable recordings. All graph representations display the fEPSPs slope (in millivolts per millisecond)/PFV (in millivolts per millisecond), which is the index of synaptic efficiency.

HPLC Analysis. Coronal hippocampal slices (500 μm thick) from neonates (P9–P10; $n = 4$) and 3-mo-old rats ($n = 4$) were prepared as previously described for electrophysiological recordings. Individual slices were then placed inside a dish containing oxygenated ACSF where CA1 and DG areas were isolated by microdissection using a binocular microscope (Zeiss; Stemi 2000). CA1 and DG subregions from one animal were collected and then treated with 5% (wt/vol) trichloroacetic acid to extract free amino acids before HPLC analysis as previously described (60).

Western Blot Analysis. Immunoblotting analysis of whole hippocampi, microdissected CA1 and DG areas from neonates (P9–P10; $n = 6$) and adult (P60–P90; $n = 7$–9) rats was performed as described previously (7). Briefly, whole hippocampi, CA1 and DG areas were sonicated in ice-cold lysis buffer and centrifuged 10 min at 1,500 × g to remove the crude nuclear pellet. Protein extracts (30 μg per lane) were subjected to electrophoresis [8% or 10% (vol/vol) SDS-polyacrylamide gel] and electroblotted onto nitrocellulose membranes (0.2 μm; Pall Life Science). Immunodetection was accomplished by enhanced chemiluminescence (ECL) using the ECL Prime Western Blotting Detection Reagent (Amersham Biosciences). Molecular sizes were estimated by separating prestained molecular weight markers (10.5–175 kDa) in parallel (Nippon Genetics). Primary and secondary antibodies and their dilutions are listed in Table S1. Digital images of the chemiluminescent blots were captured using the GBOX system (Syngene) with the GeneSys image acquisition software. Intensity of chemiluminescent signals of the targeted protein was quantified using the gel analysis tools of ImageJ 1.47V software (National Institutes of Health).

Statistical Analysis. Data were collected and analyzed using GraphPad Prism 4.0 software for statistical analysis. All values represent mean ± SEM. Immunoblot and HPLC results were analyzed using one-way ANOVA followed by Student–Newman–Keuls multiple-comparison test for significant F values. Analysis of electrophysiological results was performed using two-way ANOVA followed by Bonferroni post hoc test (for input–output curves) and Student t test. Significance was assessed at $P < 0.05$. Symbols used are as follows: *$P < 0.05$, **$P < 0.01$, and ***$P < 0.001$.

1. Sanz-Clemente A, Nicoll RA, Roche KW (2013) Diversity in NMDA receptor composition: Many regulators, many consequences. *Neuroscientist* 19(1):62–75.
2. Collingridge GL, et al. (2013) The NMDA receptor as a target for cognitive enhancement. *Neuropharmacology* 64:13–26.
3. Paoletti P, Bellone C, Zhou Q (2013) NMDA receptor subunit diversity: Impact on receptor properties, synaptic plasticity and disease. *Nat Rev Neurosci* 14(6): 383–400.
4. Traynelis SF, et al. (2010) Glutamate receptor ion channels: Structure, regulation, and function. *Pharmacol Rev* 62(3):405–496.
5. Johnson JW, Ascher P (1987) Glycine potentiates the NMDA response in cultured mouse brain neurons. *Nature* 325(6104):529–531.
6. Kleckner NW, Dingledine R (1988) Requirement for glycine in activation of NMDA-receptors expressed in *Xenopus* oocytes. *Science* 241(4867):835–837.
7. Wolosker H, Blackshaw S, Snyder SH (1999) Serine racemase: A glial enzyme synthesizing D-serine to regulate glutamate-*N*-methyl-D-aspartate neurotransmission. *Proc Natl Acad Sci USA* 96(23):13409–13414.
8. Billard J-M (2012) D-Amino acids in brain neurotransmission and synaptic plasticity. *Amino Acids* 43(5):1851–1860.
9. Rosenberg D, et al. (2013) Neuronal D-serine and glycine release via the Asc-1 transporter regulates NMDA receptor-dependent synaptic activity. *J Neurosci* 33(8):3533–3544.
10. Papouin T, et al. (2012) Synaptic and extrasynaptic NMDA receptors are gated by different endogenous coagonists. *Cell* 150(3):633–646.
11. Li Y, et al. (2013) Identity of endogenous NMDAR glycine site agonist in amygdala is determined by synaptic activity level. *Nat Commun* 4:1760–1770.
12. Quinlan EM, Philpot BD, Huganir RL, Bear MF (1999) Rapid, experience-dependent expression of synaptic NMDA receptors in visual cortex in vivo. *Nat Neurosci* 2(4): 352–357.
13. Rodenas-Ruano A, Chávez AE, Cossio MJ, Castillo PE, Zukin RS (2012) REST-dependent epigenetic remodeling promotes the developmental switch in synaptic NMDA receptors. *Nat Neurosci* 15(10):1382–1390.
14. Williams K, Russell SL, Shen YM, Molinoff PB (1993) Developmental switch in the expression of NMDA receptors occurs in vivo and in vitro. *Neuron* 10(2):267–278.
15. Rosini E, et al. (2014) Novel biosensors based on optimized glycine oxidase. *FEBS J* 281(15):3460–3472.
16. Fossat P, et al. (2012) Glial D-serine gates NMDA receptors at excitatory synapses in prefrontal cortex. *Cereb Cortex* 22(3):595–606.
17. Mothet JP, et al. (2006) A critical role for the glial-derived neuromodulator D-serine in the age-related deficits of cellular mechanisms of learning and memory. *Aging Cell* 5(3):267–274.
18. Yang Y, et al. (2003) Contribution of astrocytes to hippocampal long-term potentiation through release of D-serine. *Proc Natl Acad Sci USA* 100(25):15194–15199.

www.manaraa.com

19. Balu DT, et al. (2013) Multiple risk pathways for schizophrenia converge in serine racemase knockout mice, a mouse model of NMDA receptor hypofunction. *Proc Natl Acad Sci USA* 110(26):E2400–E2409.

20. Coultrap SJ, Nixon KM, Alvestad RM, Valenzuela CF, Browning MD (2005) Differential expression of NMDA receptor subunits and splice variants among the CA1, CA3 and dentate gyrus of the adult rat. *Brain Res Mol Brain Res* 135(1-2):104–111.

21. Morishita W, et al. (2007) Activation of NR2B-containing NMDA receptors is not required for NMDA receptor-dependent long-term depression. *Neuropharmacology* 52(1):71–76.

22. Paoletti P, Ascher P, Neyton J (1997) High-affinity zinc inhibition of NMDA NR1-NR2A receptors. *J Neurosci* 17(15):5711–5725.

23. Volianskis A, et al. (2013) Different NMDA receptor subtypes mediate induction of long-term potentiation and two forms of short-term potentiation at CA1 synapses in rat hippocampus in vitro. *J Physiol* 591(Pt 4):955–972.

24. Chen PE, et al. (2008) Modulation of glycine potency in rat recombinant NMDA receptors containing chimeric NR2A/2D subunits expressed in *Xenopus laevis* oocytes. *J Physiol* 586(1):227–245.

25. Priestley T, et al. (1995) Pharmacological properties of recombinant human *N*-methyl-D-aspartate receptors comprising NR1a/NR2A and NR1a/NR2B subunit assemblies expressed in permanently transfected mouse fibroblast cells. *Mol Pharmacol* 48(5):841–848.

26. Sacchi S, Caldinelli L, Cappelletti P, Pollegioni L, Molla G (2012) Structure-function relationships in human D-amino acid oxidase. *Amino Acids* 43(5):1833–1850.

27. Ferraris D, et al. (2008) Synthesis and biological evaluation of D-amino acid oxidase inhibitors. *J Med Chem* 51(12):3357–3359.

28. Puyal J, Martineau M, Mothet J-P, Nicolas M-T, Raymond J (2006) Changes in D-serine levels and localization during postnatal development of the rat vestibular nuclei. *J Comp Neurol* 497(4):610–621.

29. Wang L-Z, Zhu X-Z (2003) Spatiotemporal relationships among D-serine, serine racemase, and D-amino acid oxidase during mouse postnatal development. *Acta Pharmacol Sin* 24(10):965–974.

30. Henneberger C, Papouin T, Oliet SHR, Rusakov DA (2010) Long-term potentiation depends on release of D-serine from astrocytes. *Nature* 463(7278):232–236.

31. Perea G, Navarrete M, Araque A (2009) Tripartite synapses: Astrocytes process and control synaptic information. *Trends Neurosci* 32(8):421–431.

32. Ehmsen JT, et al. (2013) D-Serine in glia and neurons derives from 3-phosphoglycerate dehydrogenase. *J Neurosci* 33(30):12464–12469.

33. Martineau M, Parpura V, Mothet J-P (2014) Cell-type specific mechanisms of D-serine uptake and release in the brain. *Front Synaptic Neurosci* 6(12):1–9.

34. Andersson M, Blomstrand F, Hanse E (2007) Astrocytes play a critical role in transient heterosynaptic depression in the rat hippocampal CA1 region. *J Physiol* 585(Pt 3):843–852.

35. Martina M, et al. (2005) Reduced glycine transporter type 1 expression leads to major changes in glutamatergic neurotransmission of CA1 hippocampal neurones in mice. *J Physiol* 563(Pt 3):777–793.

36. Zafra F, Gomeza J, Olivares L, Aragón C, Giménez C (1995) Regional distribution and developmental variation of the glycine transporters GLYT1 and GLYT2 in the rat CNS. *Eur J Neurosci* 7(6):1342–1352.

37. Potier B, et al. (2010) Contribution of the D-serine-dependent pathway to the cellular mechanisms underlying cognitive aging. *Front Aging Neurosci* 2(1):1–11.

38. Laruelle M (2014) Schizophrenia: From dopaminergic to glutamatergic interventions. *Curr Opin Pharmacol* 14:97–102.

39. Gambrill AC, Barria A (2011) NMDA receptor subunit composition controls synaptogenesis and synapse stabilization. *Proc Natl Acad Sci USA* 108(14):5855–5860.

40. Pérez-Otaño I, Ehlers MD (2004) Learning from NMDA receptor trafficking: Clues to the development and maturation of glutamatergic synapses. *Neurosignals* 13(4):175–189.

41. Matsui T, et al. (1995) Functional comparison of D-serine and glycine in rodents: The effect on cloned NMDA receptors and the extracellular concentration. *J Neurochem* 65(1):454–458.

42. Panatier A, et al. (2006) Glia-derived D-serine controls NMDA receptor activity and synaptic memory. *Cell* 125(4):775–784.

43. Hansen KB, Ogden KK, Yuan H, Traynelis SF (2014) Distinct functional and pharmacological properties of triheteromeric GluN1/GluN2A/GluN2B NMDA receptors. *Neuron* 81(5):1084–1096.

44. Tovar KR, McGinley MJ, Westbrook GL (2013) Triheteromeric NMDA receptors at hippocampal synapses. *J Neurosci* 33(21):9150–9160.

45. Hashimoto A, Oka T, Nishikawa T (1995) Anatomical distribution and postnatal changes in endogenous free D-aspartate and D-serine in rat brain and periphery. *Eur J Neurosci* 7(8):1657–1663.

46. Schell MJ, Brady RO, Jr, Molliver ME, Snyder SH (1997) D-Serine as a neuromodulator: Regional and developmental localizations in rat brain glia resemble NMDA receptors. *J Neurosci* 17(5):1604–1615.

47. Kartvelishvily E, Shleper M, Balan L, Dumin E, Wolosker H (2006) Neuron-derived D-serine release provides a novel means to activate *N*-methyl-D-aspartate receptors. *J Biol Chem* 281(20):14151–14162.

48. Romero GE, Lockridge AD, Morgans CW, Bandyopadhyay D, Miller RF (2014) The postnatal development of D-serine in the retinas of two mouse strains, including a mutant mouse with a deficiency in D-amino acid oxidase and a serine racemase knockout mouse. *ACS Chem Neurosci* 5(9):848–854.

49. Song Y, et al. (2008) D-Amino acids in rat brain measured by liquid chromatography/ tandem mass spectrometry. *Neurosci Lett* 445(1):53–57.

50. Balu DT, Coyle JT (2011) Glutamate receptor composition of the post-synaptic density is altered in genetic mouse models of NMDA receptor hypo- and hyperfunction. *Brain Res* 1392:1–7.

51. Burnet PWJ, et al. (2011) D-Amino acid oxidase knockdown in the mouse cerebellum reduces NR2A mRNA. *Mol Cell Neurosci* 46(1):167–175.

52. Nong Y, et al. (2003) Glycine binding primes NMDA receptor internalization. *Nature* 422(6929):302–307.

53. Martineau M, et al. (2013) Storage and uptake of D-serine into astrocytic synaptic-like vesicles specify gliotransmission. *J Neurosci* 33(8):3413–3423.

54. Mothet J-P, et al. (2005) Glutamate receptor activation triggers a calcium-dependent and SNARE protein-dependent release of the gliotransmitter D-serine. *Proc Natl Acad Sci USA* 102(15):5606–5611.

55. Raiteri L, et al. (2008) Functional expression of release-regulating glycine transporters GLYT1 on GABAergic neurons and GLYT2 on astrocytes in mouse spinal cord. *Neurochem Int* 52(1-2):103–112.

56. Sakata K, et al. (1997) Characterization of glycine release mediated by glycine transporter 1 stably expressed in HEK-293 cells. *Brain Res Mol Brain Res* 49(1-2):89–94.

57. Yang Y, Higashimori H, Morel L (2013) Developmental maturation of astrocytes and pathogenesis of neurodevelopmental disorders. *J Neurodev Disord* 5(22):1–8.

58. Aimone JB, et al. (2014) Regulation and function of adult neurogenesis: From genes to cognition. *Physiol Rev* 94(4):991–1026.

59. Labarrière M, et al. (2014) Circuit-specific changes in D-serine-dependent activation of the *N*-methyl-D-aspartate receptor in the aging hippocampus. *Age (Dordr)* 36(5):9698–9709.

60. Curcio L, et al. (2013) Reduced D-serine levels in the nucleus accumbens of cocaine-treated rats hinder the induction of NMDA receptor-dependent synaptic plasticity. *Brain* 136(Pt 4):1216–1230.

Le Bail et al.

www.manaraa.com